HHS Public Access

Author manuscript

Cancer Res. Author manuscript; available in PMC 2019 May 29.

Published in final edited form as:

Cancer Res. 2018 December 01; 78(23): 6680–6690. doi:10.1158/0008-5472.CAN-17-3878.

The TLR7/8/9 antagonist IMO-8503 inhibits cancer-induced cachexia

Federica Calore[1], **Priya Londhe**[1], **Paolo Fadda**[1], **Giovanni Nigita**[1], **Lucia Casadei**[2,3], **Gioacchino Paolo Marceca**[1,4], **Matteo Fassan**[5], **Francesca Lovat**[1], **Pierluigi Gasparini**[1], **Lara Rizzotto**[6], **Nicola Zanesi**[1], **Devine Jackson**[1], **Svasti Mehta**[1], **Patrick Nana-Sinkam**[7], **Deepa Sampath**[6], **Raphael E. Pollock**[2,3], **Denis C. Guttridge**[1], and **Carlo M. Croce**[1]

[1.]Department of Cancer Biology and Genetics and Comprehensive Cancer Center, The Ohio State University, Columbus, OH 43210.

[2.]The James Comprehensive Cancer Center, The Ohio State University, Columbus, Ohio.

[3.]Department of Surgery, Division of Surgical Oncology, The Ohio State University Wexner Medical Center, Columbus, Ohio.

[4.]Bioinformatics Unit, Department of Clinical and Experimental Medicine, University of Catania, c/o Dipartimento di Matematica e Informatica, Viale A. Doria 6, 95125 Catania, Italy.

[5.]Department of Medicine, Surgical Pathology & Cytopathology Unit, University of Padua, via Giustiniani 2, 35128 Padua, Italy.

[6.]Division of Hematology, The Ohio State University Comprehensive Cancer Center, Columbus, OH 43210.

[7.]Division of Pulmonary Disease and Critical Care Medicine, Virginia Commonwealth University, VA 23298.

Abstract

Muscle wasting is a feature of the cachexia syndrome, which contributes significantly to cancer patient mortality. We have previously demonstrated that miR-21 is secreted through extracellular vesicles (EVs) by lung and pancreatic cancer cells and promotes JNK-dependent cell death through its binding to the *TLR7* receptor in murine myoblasts. Here we evaluate the ability of IMO-8503, a TLR7, 8 and 9 antagonist, to inhibit cancer-induced cachexia. Using EVs isolated from lung and pancreatic cancer cells and from patient plasma samples, we demonstrate that IMO-8503 inhibits cell death induced by circulating miRNAs with no significant toxicity. Intraperitoneal administration of the antagonist in a murine model for Lewis Lung Carcinoma (LLC-induced cachexia) strongly impaired several cachexia-related features, such as expression of Pax7 as well as caspase 3 and PARP cleavage in skeletal muscles, and significantly prevented the

Corresponding Authors: Carlo M. Croce, 1082 Biomedical Research Tower, 460 W 12th Avenue, Columbus 43210 OH USA; Phone: (+1) 614-292-4930; Fax (+1) 614-292-3358; carlo.croce@osumc.edu, and Denis C. Guttridge, 520 Biomedical Research Tower, 460 W 12th Avenue, Columbus 43210 OH USA; Phone: (+1) 614-688-3137; Fax: (+1) 614-292-6356; guttridg@musc.edu.

Disclaimers: None reported.

All authors declare no potential conflicts of interest.

loss of lean mass in tumor-bearing mice. IMO-8503 also impaired circulating miRNA-induced cell death in human primary myoblasts.

Taken together, our findings strongly indicate that IMO-8503 serves as a potential therapy for the treatment of cancer cachexia.

Precis

Cancer-associated cachexia is a significant problem for cancer patients that remain poorly understood, understudied, and inadequately treated. Findings report a potential new therapeutic for the treatment of *TLR7*-mediated cancer cachexia.

Keywords

microRNAs; cachexia; cachexia mouse model; Extracellular Vesicles; cancer; TLR inhibitor; cachexia treatment; myoblasts

INTRODUCTION

Cachexia is a multifactorial and highly debilitating syndrome characterized by weight loss which results from the reduction of skeletal muscle tissue mass, with or without loss of fat mass (1). Such pathological condition has been associated with many types of chronic diseases, including cancer (2). In cancer patients, the main symptoms associated with cachexia are asthenia, physical illness, and fatigue. Moreover, in advanced cancer more than 50% of patients display cachectic symptoms, especially in pancreatic and lung cancer, and nearly 20% of cancer-related mortalities occur because of cachexia rather than tumor burden (3). Since several factors concur in the onset of cachexia and the mechanisms involved have not been fully elucidated, the pathophysiology of this syndrome is still unclear. Previously, we showed that miR-21 secreted through extracellular vesicles (EVs) by lung and pancreatic cancer cells contributes to muscle loss associated with cancer cachexia (4). This occurred by induction of apoptosis in murine myoblasts through the binding of miR-21 to the Toll-like receptor 7 (*TLR7*) and by activation of JNK (4). Indeed, we demonstrated that lung cancer EV-secreted miR-21 and miR-29a are also capable to bind to human Toll-like receptor 8 (TLR8, whose murine orthologue is *TLR7*) within surrounding macrophages leading to a pro-metastatic inflammatory response via the NF-κB pathway (5). TLR7/8 belong to the Toll-like receptor family, a group of transmembrane receptors that have a pivotal role in the regulation of innate immune defense against pathogens. TLR8, along with TLR3, 7 and 9, are localized in endosomes and recognize non-self nucleic acids, including pathogen-derived nucleic acid molecular patterns (6). TLR3 recognizes double-stranded RNA molecules (7), while TLR7 and 8 bind single-stranded RNA (8), and TLR9 recognizes unmethylated DNA with CpG-motifs (9).

In this study, we investigated the role of IMO-8503, a TLR7, 8 and 9 antagonist (Analogue of IMO-8400, a clinical candidate for dermatomyositis, Clinicaltrials.gov ID: NCT02612857), in the cell death response of murine myoblasts induced by lung and pancreatic cancer-derived EVs. Our findings demonstrate that IMO-8503 significantly impairs killing triggered by synthetic miR-21 oligo and by EVs derived from cancer cell

lines or lung and pancreatic patient plasma samples. Also, the antagonist was shown to be effective in the inhibition of apoptosis induced by miR-29a, which promoted cell death more strongly than miR-21. These findings were then confirmed by using human primary myoblasts in an *in vitro* experiment.

In vitro, IMO-8503 inhibited JNK signaling-mediated cell death in C2C12 myoblasts through the competitive binding to *TLR7*. *In vivo*, tumor-bearing mice treated with the antagonist showed impaired expression of the stem cell self-renewing transcription factor Pax7, whose upregulation was recently identified in murine models and patient samples as a cachexia marker (10,4). Moreover, treatment with IMO-8503 significantly impaired the lung cancer-dependent loss of lean mass and the cleavage of pro-apoptotic proteins Caspase 3 and PARP. These findings were supported by the analysis of murine muscle weight and food and energy intake. Conversely, we demonstrated that IMO-8503 had no effect on tumor growth.

Our data provide evidence for the development of a new treatment for cancer cachexia, and suggest that this TLR antagonist may serve as a potential therapeutic for the management of this syndrome associated with malignant tumors.

MATERIALS AND METHODS

Cell Culture.

All cell lines were purchased from American Type Culture Collection unless indicated otherwise. Murine C2C12 and human pancreatic cancer MIA PaCa-2 cells were cultured using standard conditions and were grown in DMEM (Sigma-Aldrich), supplemented with 10% (vol/vol) FBS (Sigma-Aldrich) and 1% (vol/vol) penicillin/streptomycin (Sigma), and incubated at 37 C with 5% CO2. Murine LLC (Lewis Lung Carcinoma), C26 and human pancreatic cancer AsPC1 cells were grown in RPMI 1640 (Sigma-Aldrich), supplemented with 10% (vol/vol) FBS (Sigma-Aldrich) and 1% (vol/vol) penicillin/streptomycin (Sigma), and incubated at 37 C with 5% CO2. Human HEKBlue-TLR8 293 cells (indicated as genetically modified HEK-293) were purchased from Invivogen and maintained in DMEM (Sigma-Aldrich) supplemented with 10% (vol/vol) FBS (Sigma-Aldrich), 1% (vol/vol) penicillin/streptomycin (Sigma), Normocin (50 μg/ml), Blasticidin (10 μg/ml), and Zeocin (100 μg/ml). Human Skeletal Muscle Myoblast Cells (HSMM) were purchased from Lonza and maintained in SkGM-2 medium. HSMM and HEKBlue-TLR8 were purchased within 6 months from manuscript submission and they were both thoroughly tested and validated by Lonza and Invivogen, respectively. Human AsPC1 and MIA PaCa-2 cells were validated by STR analysis in July 2018.

LLC and C26 cell lines are authenticated in the Guttridge laboratory when they produce similar cachexia to our previously published work. We recently published that our cell lines have maintained their cachexia-inducing phenotype over the last 10 years0 (11). Additional *Mycoplasma* testing has been conducted at a minimum of every six months.

IMO-8503.

IMO-8503 (5’-CAATCTGUC*G1TTCACTGU-3’, C*=5-Me-dC, G1=7-deaza-dG), the TLR7, 8 and 9 antagonist, was provided by IDERA Pharmaceuticals (Cambridge, MA

02139) and resuspended in PBS (Sigma-Aldrich). For all experiments IMO-8503 was diluted in serum-free medium to the desired concentration.

Treatments.

For the experiments with synthetic miR-16, miR-21 and miR-29a, oligos were complexed with Dotap Liposomal Transfection Reagent (Roche) following the manufacturer's instructions. Myoblasts were further treated with Dotap formulations and different concentrations of IMO-8503 together for the indicated time points.

EV isolation.

LLC- derived EVs were isolated from 250×10^6 cells cultured for 48h in Serum-free medium and prepared as described in He W., Calore F. (4). EV pellet was finally resuspended in 1 ml of serum-free medium (Invitrogen) unless indicated otherwise and used for treatments.

Animals.

40 wild type C57BL/6J mice were purchased from Jackson Laboratories. All animals were housed in Plexiglas cages, each of them containing 4 mice according to standard laboratory conditions. All mice had free access to standard chow and water.

Mice, matched for age and sex (females, 7 week-old) were divided into 6 groups:

"Group A": negative control group. Mice from this group were NOT injected with tumor cells nor treated with IMO-8503 for the whole experiment.

"Group B": mice from this group were not inoculated with LLC cells, but were treated with IMO-8503 (25 mg/kg/mouse, IP injection) every two days.

"Group C": mice from this group were injected with LLC cells, but were not treated with IMO-8503.

"Group D": mice from this group were injected with tumor cells. From the day after LLC inoculation they were treated with IMO-8503 (5 mg/kg/mouse, IP injection) every two days.

"Group E": mice from this group were injected with tumor cells. From the day after LLC inoculation they were treated with IMO-8503 (25 mg/kg/mouse, IP injection) every two days.

"Group F": mice from this group were injected with tumor cells. Starting 10 days after LLC inoculation they received IMO-8503 treatment (25 mg/kg/mouse, IP injection) every two days.

Groups C, D, E and F received LLC injection (50,000 cells/mouse) on Day 0. Groups B, D and E were treated with the indicated concentration of IMO-8503 starting on Day 1, while group F received the treatment starting on Day 10 (see Fig. 5A).

Mice were followed for survival and after 21 days from tumor cells injection they were sacrificed. Quadriceps, tibialis anterior and gastrocnemius muscles were then collected, weighed and frozen. Part of the gastrocnemius samples were cut into smaller pieces for whole mount immunohistochemistry, while the remaining part was further processed by tissue homogenization for western blot and real-time PCR analysis.

All procedures in this study complied with federal guidelines and institutional policies by The Ohio State University animal care and use committee. Our study was approved by the Institutional Animal Care and Use Committee (IACUC).

Mice assessment.

Mice weight was recorded starting on Day 1 twice/week by using an electronic scale. Tumor growth was checked twice/week. A weighed aliquot of food (200 g/cage) was changed on a weekly basis. Food intake was assessed two times/week by subtracting the remaining amount of food from the initial dose. Energy intake was determined on the basis of 3.1 kcal/g (13.0 kJ/g) of standard chow. Final body length was assessed by measuring nasal-to-anal distance using a caliper at the moment of sacrifice.

Body composition.—Body composition was assessed through EchoMRI Analysis (EchoMRI 3-in-1 v2.1; Echo Medical Systems, Houston, TX), that accurately measures lean, fat, free water and total water masses in live animals. Mice were scanned 12 hours prior to being euthanized. Animals did not receive anesthesia nor special preparation before measurement. Scanning took up to 5 minutes per mouse.

Lean Mass and (Lean + Fat) Mass Index.—Lean Mass Index (LMI) was assessed by using the formula $(LM)/l^2$, where LM corresponds to the lean mass (g) determined through EchoMRI, while l corresponds to the body length of the animal in cm^2. The (Lean + Fat) Mass Index (LMFI), instead, was determined by using the formula $(LM + FM)/l^2$, where (LM + FM) corresponds to the lean and fat masses assessed by EchoMRI, while l corresponds to the body length of the animal in cm^2.

Tumor weight.—When mice were sacrificed, all tumors were removed from carcasses and weighed by using an electronic precision scale.

Immunohistochemistry.

Immunohistochemistry analysis was performed as described in Casadei L., Calore F. et al. (12). Samples were stained with anti-cleaved Caspase 3 (Abcam) and then analyzed.

Statistical analysis.

Statistical data are presented as mean ± standard deviation. Statistical significances were calculated by using *stats* R package, in particular: analyses between two groups were performed by using a two-tailed Student's t-test, while one-way, two-way ANOVA tests and Kruskal-Wallis rank sum test were applied for multiple-factorial designs. Pearson's correlation analyses, together with scatter plots, were performed using the function *ggscatter* in the *ggpubr* R package.

RESULTS

IMO-8503 impairs human TLR8 activation.

In order to determine the impact of IMO-8503 on the activation of the TLR7/8 receptor induced by secreted miRNAs, we treated genetically modified HEK-293 cells that stably overexpressed human TLR8 with a Dotap formulation of miR-21 (therefore mimicking vesicle-secreted miR-21) in the presence of different concentrations of the antagonist. After 24h, we performed an NF-κB reporter assay that assessed whether the receptor was activated by a specific molecule through a colorimetric test (Fig. 1). Our results indicate that IMO-8503 significantly impaired TLR8 activation induced by miR-21 in a dose-dependent fashion ($P < 2e^{-16}$). When IMO-8503 was used at a concentration of 30 μM the activation of human TLR8 was impaired by 82%.

IMO-8503 protects myoblasts by circulating miRNA-induced cell death.

To investigate the ability of IMO-8503 to impair cell death induced by miR-21 on murine myoblasts, we treated C2C12 cells with Dotap alone or a Dotap formulation of miR-21 in the presence of different concentrations of the antagonist. In order to exclude any possible toxic effect of the molecule itself on the cells, as a control, we treated C2C12 cells with different concentrations of IMO-8503 only. Moreover, since we had previously demonstrated that secreted miR-29a also binds and activates the TLR7/8 receptor (5) we checked whether, similarly to miR-21, miR-29a also promoted C2C12 cell death. Hence, we incubated myoblasts with a Dotap formulation of miR-29a in the same conditions described above. We then assessed the number of viable proliferating C2C12 cells 24 and 48h after treatments. At first we observed that miR-29a induced cell death, in a similar manner to miR-21. When used alone with no antagonist added, miR-29a had a similar impact on C2C12 viability to miR-21 at 24h (Fig. 2, compare panels A and B). However, at 48h the effect of miR-29a was much more dramatic and the IMO-8503 protection from cell death was lower when compared with the miR-21 counterpart. These data therefore indicate that in addition to miR-21, tumor-secreted miR-29a induces a significant pro-cachectic effect in our model (Fig. 2C, D). Moreover, IMO-8503 itself was toxic on C2C12 cells when used at a concentration of 15, 30 and 40 μM, as its effects were comparable to those obtained by the combination of miR-21/29a plus IMO-8503 at the same concentrations (Fig. 2A, B). Considering these findings, we determined that an antagonist concentration of 7.5 μM was suitable to impair cell death induced by synthetic miR-21 and miR-29a, as it reduced the effects of both miRNAs while not being toxic for cells at both time points (Fig. 2).

In order to validate our data, we treated C2C12 cells either with synthetic oligos or with LLC-derived EVs in the presence or absence of IMO-8503. The results confirmed our preliminary findings that IMO-8503 significantly protected myoblasts from cell death when they were treated with either synthetic miR-21 or miR-29a or when they were incubated with Lewis Lung Carcinoma (LLC)-derived EVs (compare Fig. 3A and B, C and D, E and F).

The LLC model is an established and validated mouse model of cachexia (13). This indicated that IMO-8503 significantly protects myoblasts from miRNA-induced toxicity

with little or no toxic side effect on the cells themselves. We used primary human skeletal muscle cells to recapitulate out murine data: in human primary skeletal muscle cells IMO-8503 significantly impaired cell death induced by synthetic miR-21 and miR-29a (Supplemental Fig. S1 A), and also protected human primary myoblasts from the killing action of LLC-derived EVs (Supplemental Fig. S1B). Furthermore, we incubated human primary myoblasts with human pancreatic cancer-derived EVs from AsPC1 and MIA PaCa-2 cell lines. After a 40h incubation with isolated particles, myoblast viability was strongly affected, while the same parameter was significant rescued by treatment with the TLR inhibitor (Supplemental Figure S1C and D), indicating that the anti-cachectic action of IMO-8503 could be effective in patients affected by lung and pancreatic cancer.

To further strengthen our *in vitro* results, we isolated EVs from the plasma of pancreatic and lung cancer patients, assessed their quality by Nanosight analysis and excluded the possibility of cell contamination (Supplemental Fig. S2). We next incubated murine myoblasts with isolated particles for 24h. In parallel, cells were treated with EVs isolated by the same plasma samples in the presence of IMO-8503. Results showed that pancreatic cancer-derived EVs induced considerably higher apoptosis levels compared to those induced by EVs isolated from healthy donors (Fig. 4A). EVs derived from lung cancer plasma samples exhibited a similar cell-killing activity in comparison to those derived by healthy donors (Fig. 4B, patient detailed information is reported in Supplemental Table S1). However, as seen in our previous findings, incubation with IMO-8503 significantly impaired cell death ($0.01 < P \leq 0.05$ and $0.001 < P \leq 0.01$) (Fig. 4).

In tumor-bearing mice, IMO-8503 significantly attenuates cachectic phenomenon.

We next evaluated IMO-8503 *in vivo*. For this purpose, we injected LLC cells into C57/B6 mice, and one day post-injection administered IMO-8503. Treatment was repeated every two days at two different doses, 5 and 25 mg/kg/mouse. A third group was treated with the higher dose of antagonist starting 10 days post tumor cell injection, while LLC-injected mice treated with PBS were used as positive control for cachexia. We also included a non-injected group (no LLC, no IMO-8503) as a negative control, and a group of mice that did not receive LLC cells, but were treated with the higher dose of IMO-8503 only (Fig. 5A). For three weeks we recorded several parameters such as body weight and food intake. We then assessed body composition of all animals, in order to determine the amount of their lean, fat, free water and total water masses, and after 12h mice were sacrificed. Quadriceps, tibialis anterior and gastrocnemius muscles were collected and weighed as well as tumor masses. Gastrocnemius muscles were further processed for immunohistochemistry, real-time PCR and western blot analysis, in order to assess the expression levels of different proteins, such as the cachectic marker Pax7 (10). As expected, the presence of Pax7 was clearly detected within the Positive Control group (“Group C”), and was reduced in the Negative Control group (“Group A”). Interestingly, Pax7 presence was strongly impaired in the groups that received IMO-8503 treatment, either in the 5 mg/kg (“Group D”) or in the 25mg/kg dose group (“Group E”). Similarly, Pax7 was downregulated within the group of mice whose treatments with IMO-8503 had been initiated 10 days post tumor cell injection (“Group F”) (Fig. 5B), indicating that protection from the TLR7, 8 and 9 antagonist is effective even when tumor growth is progressing. Moreover, we noticed that in the group

that was not injected with LLC cells but received the higher dose of IMO-8503 (“Group B”) the expression of Pax7 was higher with respect to the negative control group (“Group A”), suggesting that the administration of the TLR antagonist 25 mg/kg/mouse for three weeks could result toxicity (Fig. 5B, western blot lower panel). Within the same samples, MyoD was negatively regulated with respect to Pax7 overexpression, confirming that Pax7 induces wasting by suppressing MyoD (10).

Since our previous findings demonstrated that the cell death of myoblasts induced by secreted miR-21 is mediated by the phospho-JNK pathway, we further verified whether IMO-8503 inhibited the activation of such pathway within isolated muscles. As expected, JNK was found highly phosphorylated in the positive control group for cachexia (“Group C”), while decreased phosphorylation levels were observed in the remaining mice, confirming our hypothesis. Finally, the group of mice that received the TLR antagonist treatment 10 days after LLC injection (“Group F”) showed more JNK phosphorylation with respect to other treated mice, indicating that delayed administration of IMO-8503 was enough to impair Pax7 expression, but not to activate the phospho-JNK pathway (Fig. 5B). No differential phosphorylation of p38 was detected.

Likewise, body composition findings were in line with the *in vivo* data. Both the Lean Mass and the (Lean + Fat) Mass Index (LMI and LFMI, respectively) we calculated for all groups of mice were strongly reduced in the Positive Control group for cachexia (“Group C”) with respect to the un-injected group (“Group A”). Surprisingly, when mice were treated with the lower dose of IMO-8503 (5 mg/kg/mouse, “Group D”), the lean mass loss was impaired (Fig. 5C). Interestingly, the loss for the group of mice that were treated with the TLR antagonist only (“Group B”) was similar to our positive control (“Group C”), once again suggesting that a 25 mg/kg/mouse dosage of IMO-8503 was toxic for the animals. Similarly to the “Group B”, the combination of the injection of tumor cells and high dose of IMO-8503 was not sufficient to impair muscle loss in Groups E and F (Fig. 5C), although Pax7 expression was reduced in those groups. We suspect that this occurs because of an interplay of several other factors that can contribute to cachexia.

The effect of IMO-8503 on JNK phosphorylation was further confirmed by *in vitro* experiment on C2C12 cells incubated with LLC-derived EVs, in the presence or absence of IMO-8503 7.5 μM for different time points. Western blot analysis showed that IMO-8503 successfully impaired the phosphorylation of JNK induced by EVs. (Fig. 6).

Analysis of muscle for all the three different isolated muscle types (quadriceps (QUAD), tibialis anterior (TA) and gastrocnemius (GAST)), revealed that “Group C” samples was characterized by major loss of lean mass with respect to the negative control (“Group A”). Differently, when mice were treated with IMO-8503 5 mg/kg/mouse an impaired loss of weight for TA and GAST was recorded (Supplemental Fig. S3). The Kruskal-Wallis rank sum test indicated that these findings were not statistically significant, however their trend support results from the *in vivo* experiment and body composition analysis.

Since during the *in vivo* experiment we recorded both the food intake and mouse weight per group, we next plotted the body weight increase with respect to the average daily energy

intake. Our negative control for cachexia, “Group A”, showed no correlation (r= 0.029) (Supplemental Fig. S4A), while mice injected with LLC cells, but not treated with IMO-8503, presented a negative correlation, although not significant (“Group C”, r= − 0.19, *P*= 0.26). Surprisingly, when tumor-bearing mice were injected with IMO-8503 5 mg/kg/mouse (“Group D”) there was still no correlation (r= 0.0082), supporting our previous *in vivo* findings and suggesting that the lower dose of TLR antagonist sufficiently impaired the cachexia features displayed by our positive control group. Interestingly, “Group E” and “Group F” displayed a negative correlation, suggesting that the tumor together with a dose of 25 mg/kg/mouse were somehow harmful for the animals, apparently in a synergetic manner. Similarly to the negative control for cachexia, the IMO-8503 25 mg/kg/mouse-only group, “Group B”, showed no correlation (r= 0.027), indicating that although the TLR antagonist could result some kind of toxicity (see Pax7 expression and muscle weight, respectively Figure 5 and Supplemental Fig. S3), it did not affect the body weight gain during the experiment (Supplemental Fig. S4A). Specific food intake measurements are reported in Supplemental Table S2.

In line with these data were the conclusions regarding the energy intake per group during the three weeks of experiment: for each measurement “Group A” displayed a major energy density per mouse with respect to the remaining groups (Supplemental Fig. S4B). Similarly, the “Group B” showed an individual energy density trend above the remaining groups, indicating that a high dose of IMO-8503 did not affect the food and energy intake. For the remaining groups, results were not significant, and indicate again that IMO-8503 does not have any effect in such process.

IMO-8503 has no effect on tumor growth or autophagy.

We next asked whether the anti-cachectic role of IMO-8503 could depend on any effect on tumor cell growth. We therefore incubated LLC cells with IMO-8503 7.5 μM for 24 and 48h. The MTS assay revealed that the TLR antagonist did not influence tumor cell growth at both time points (Supplemental Fig. S5A). We further compared the weight of the tumor masses removed from all the tumor-bearing mice. As shown in Supplemental Fig. S5B, no significant difference was detected, confirming that IMO-8503 does not influence tumor growth.

In order to investigate the involvement of additional mechanisms for the anti-cachectic action of IMO-8503, we assessed the expression of various markers within isolated gastrocnemius samples, including TNFR-Associated Factor 6 (*Traf6*), a gene encoding for a protein with E3 ubiquitin ligase activity (14), Autophagy-related 5 (*Atg5*) and BCL2/adenovirus E1B 19 kDa Protein-Interacting Protein 3 (*Bnip3*), two genes that are regulated in the autophagy and programmed cell death pathways, respectively (15,16). We found that *Traf6* expression was upregulated in the positive control for cachexia group, while it was slightly downregulated in the remaining groups, as expected (Supplemental Fig. S6A). Although these data are not statistically significant, their trend sustain the anti-cachectic effect of IMO-8503.

Conversely, we did not observe significant differences between our test groups for the expression of *Atg5* and *Bnip3* (Supplemental Fig. S6B and C), suggesting that IMO-8503 does not relieve the cachectic burden by regulating autophagy or programmed cell death.

IMO-8503 impairs PARP and Caspase 3 cleavage in myoblasts.

We investigated whether IMO-8503 impaired the Caspase 3 and PARP cleavage in isolated gastrocnemius samples. The immunohistochemistry analysis revealed that Caspase 3 cleavage was more abundant in the gastrocnemius of mice inoculated only with LLC cells with respect to the un-injected group (Fig. 7A, compare “Group C” with “Group A”). Treatment with IMO-8503 5 mg/kg/mouse strongly impaired such process (Fig. 7A, “Group D”), while the higher dose of IMO-8503 only (“Group B”) or the combination of tumor cells and IMO-8503 25 mg/kg/mouse (“Groups E and F”) led to an increase of Caspase 3 cleavage with respect to the negative control group, underlying once again the toxic effect of such conditions.

Similarly, PARP cleavage was strongly impaired when mice were treated with IMO-8503 5 mg/kg/mouse (“Group D”) with respect to other injected mice (Fig. 7B and C).

These data further support our previous findings and indicate that the antagonist impairs cell death in myoblasts by inhibiting apoptosis.

Colon cancer-derived EVs have no killing activity on murine myoblasts.

Since another well-known cancer cachexia model is established from C26 colon cancer cells (17), we verified whether C26-derived EVs had the same killing effect we reported for lung and pancreatic-secreted vesicles on myoblasts.

Hence, we incubated C2C12 cells with C26-derived EVs for 24 and 48h in the presence or absence of IMO-8503 7.5 μM. Surprisingly, when we assessed cell proliferation, we noticed that colon particles did not induce cell death at both time points (Supplemental Figure S7A). Moreover, C26-derived vesicles significantly promoted cell proliferation after 24h of incubation.

In order to better understand our results, we verified the presence of miR-21 and miR-29a within isolated vesicles and determined the concentration of C26-derived EVs with respect to LLC-secreted particles. Interestingly, colon cells secreted both miRNAs (although miR-29a expression was much lower in C26-derived EVs with respect to LLC-derived EVs), and the Nanosight analysis revealed that the amount of particles secreted by both cell lines was not significantly different (Supplemental Figure S7B and C). In light of this, we speculate that colon cancer-associated cachexia could be regulated by different mechanisms with respect to lung and pancreatic tumors. For this reason, further investigation will be performed in the future.

DISCUSSION

In the present study, we have characterized IMO-8503, a new TLR7, 8 and 9 antagonist by *in vitro* and *in vivo* studies, as a potential promising therapeutic for the treatment of cancer

cachexia. Our findings strongly support that the antagonist is an effective competitor of vesicular miR-21/29a in binding the *TLR7* receptor and can significantly inhibit miRNA-mediated cell death in murine myoblasts. These data were substantiated when the antagonist was observed to impair cell death induced by pancreatic and lung cancer patient-derived EVs. Moreover, IMO-8503 was significant effective at protecting human myoblasts by the killing activity of LLC- and human pancreatic cancer cells-derived EVs, further validating its reliability as a candidate for the treatment of cachexia. *In vivo*, the TLR7, 8 and 9 antagonist had a strong impact at impairing several cachexia features displayed in tumor-bearing mice. First of all, the presence of Pax7 within our lysates was reduced in all mice treated with IMO-8503, at both low and high doses. Moreover, IMO-8503 impaired JNK phosphorylation, hence the pathway that led to cell death in circulating miRNA-dependent cachexia.

Impressively, the body composition analysis revealed that IMO-8503 significantly impaired lean and (lean + fat) mass loss in tumor bearing mice, when used at a concentration of 5 mg/kg/mouse. These data were supported by other findings, such as the muscle weight analysis, the study of food and energy intake and the analysis of Caspase 3 and PARP cleavage. Moreover, different concentrations of IMO-8503 had no impact in tumor growth in all tumor-bearing mice, underlying that the antagonist has an anti-cachectic, but not an anti-tumor role.

Surprisingly, our data showed that the higher dose which was administered to mice, 25 mg/kg/mouse, resulted in toxicity. In fact, we noticed that mice treated only with IMO-8503 expressed Pax7 within gastrocnemius lysates, and that the impact of the antagonist on lean and (lean + fat) mass loss and muscle weight produced similar effects to the positive cachexia control group of mice (e. g. see body composition analysis). However, no effect was apparently observed at the level of food and energy intake. What we believe is that the combination IMO-8503 25mg/kg/mouse and tumor had a synergistic, toxic effect. Our findings indicate that a concentration of 5 mg/kg/mouse is therefore ideal for the treatment of cachexia in mice without potential side effects.

The importance of the role of both miRNAs and tumor microenvironment in the regulation of cancer cachexia has been substantiated by recent findings showing that circulating miR-21 has an important role in myoblast apoptosis associated to cancer cachexia (4). Moreover, in this study we showed that microvesicle-secreted miR-29a promotes C2C12 cell death to a stronger extent than miR-21.

In contrast with our findings regarding the regulation of lung and pancreatic cancer cachexia, colon cancer C26-derived vesicles did not display any killing activity on murine myoblasts. Given the amount of released particles and the presence of miR-21 and miR-29a within colon-secreted EVs (although the expression of miR-29a was much lower with respect to LLC-derived EVs), we can speculate that in the C26 mouse model for cachexia the mechanisms that regulate lean mass loss may depend either on other factors in addition to extracellular vesicles. The alleged different mechanisms between lung and pancreatic cachexia versus colon cancer cachexia are consistent with the metabolic alteration similarities that have been reported for patients, whereby both lung and pancreatic cancer

patients are characterized by APP response (acute-phase proteins, production of C-reactive protein and fibrinogen) (18). In addition, in the latter two types of tumors an increased resting energy expenditure (REE) was observed, differently from other cancer types, including colorectal cancer (19). For such reasons, the study of the mechanisms regulating colon cancer cachexia deserves further investigation.

To date, cancer cachexia treatments remain mostly ineffective. In the past few years myostatin inhibitors have been considered a promising therapeutic strategy. These molecules inhibit proteolytic pathways leading to muscle hypertrophy. Among these, PF-06252616 is a myostatin antibody currently in Phase I testing in healthy volunteers, while LY2495655 is in Phase II trial for pancreatic cancer. Moreover, BYM-338 is an anti-activin receptor IIB antibody that has reached Phase II for the treatment of non-small cell lung cancer patients suffering from cachexia (20).

Other cachexia treatments are drug-based. In head and neck cancer megestrol acetate and medroxyprogesterone acetate, two progestational agents, are prescribed in addition to corticosteroids. Other treatment options include nonsteroidal anabolic androgens, such as MK-2866, that have finally reached Phase III trials, and antioxidant agents or nonsteroidal anti-inflammatory drugs (21). There are also non pharmacological approaches that include nutritional strategies and exercise rehabilitation training aimed at reversing muscular metabolic abnormalities (22). In addition to these agents, we propose the inhibition of the *TLR7* receptor through an antagonist as a potential cancer cachexia treatment option to be considered for further development, at least for the lung and pancreatic cancer models.

To this point, inhibition of the TLR receptor activity has been conceived as a treatment option for inflammatory and autoimmune diseases. The mechanism of action of a TLR7, 8 and 9 receptor is different from that of monoclonal antibodies (i.e. monoclonal antibodies directed against cytokines) or immunosuppressants, as they are limited to the inhibition of a preselected, single target to induce a global inhibitory effect. Conversely, the inhibition of TLR receptors through an oligonucleotide-based antagonist can impair the production of different cytokines as a consequence of the specific involvement of the TLR7, 8 and 9 receptors. This would consequently modulate the immune response in a wider manner. For instance, IMO-3100, a TLR7 and 9 antagonist showed clinical activity in a Phase II proof-of-concept trial in moderate to severe psoriasis patients. IMO-8400 is in clinical development for dermatomyositis and, similarly to its analog IMO-8503, shows specificity to TLR7, 8 and 9 receptor, but not TLR3 or 4 (23).

Based on our current findings, we believe that the unique mechanism of action of TLR antagonist offers potential as a new therapeutic for the treatment of cachexia.

Supplementary Material

Refer to Web version on PubMed Central for supplementary material.

ACKNOWLEDGEMENTS

We thank IDERA Pharmaceuticals, in particular Dr. Wayne Jiang, for providing us the TLR7, 8 and 9 antagonist used in this study, IMO-8503.

We thank the following for their scientific and technical support: Dr. Luisa Tomasello and Nicole Zalles (from the group of Dr. Carlo Croce); and Dr. Katherine Ladner, Melissa Siebert, Dr. Erin Talbert (from the group of Dr. Denis Guttridge).

EchoMRI analysis was performed by Dr. Anna Bratasz and Michelle Williams (Small Animal Imaging Core (SAIC), Davis Heart and Lung Institute).

Alexander Ridenour and Alex Cornwell from The Ohio State University Analytical Cytometry Shared Resources provided support with Nanosight analysis.

Jason Bice from the Comparative Pathology & Mouse Phenotyping Shared Resource at OSU performed slide preparation and staining for IHC analysis.

qRT-PCR analysis was performed at The Ohio State Nucleic Acid Shared Resources (NASR).

Dr. Valerie Bergdall and Dr. Carrie Freed provided support for animal experiment.

All the Shared Resources at The Ohio State University that contributed to this paper were supported by the Cancer Center Support Grant P30CA016058.

Financial support: This work was supported by NIH CA180057 to D. C. Guttridge, R01 CA190740 to C. M. Croce and P. Nana-Sinkam and R35 CA197706 to C. M. Croce.

REFERENCES

1. Argilés JM, Busquets S, Stemmier B, López-Soriano FJ. Cancer cachexia: understanding the molecular basis. Nat Rev Cancer 2014; 14(11):754–62. [PubMed: 25291291]
2. Fearon KC, Glass DJ, Guttridge DC. Cancer cachexia: mediators, signaling, and metabolic pathways. Cell Metab 2012; 16(2):153–66. [PubMed: 22795476]
3. Acharyya S, Guttridge DC. Cancer cachexia signaling pathways continue to emerge yet much still points to the proteasome. Clin Cancer Res 2007; 13(5): 1356–61. [PubMed: 17332276]
4. He WA, Calore F, Londhe P, Canella A, Guttridge DC, Croce CM. Microvesicles containing miRNAs promote muscle cell death in cancer cachexia via TLR7. Proc Natl Acad Sci U S A 2014; 111(12):4525–29. [PubMed: 24616506]
5. Fabbri M, Paone A, Calore F, Galli R, Gaudio E, Santhanam R, et al. MicroRNAs bind to Toll-like receptors to induce prometastatic inflammatory response. Proc Natl Acad Sci U S A 2012; 109(31):E2110–16. [PubMed: 22753494]
6. Gay NJ, Symmons MF, Gangloff M, Bryant CE. Assembly and localization of Toll-like receptor signalling complexes. Nat Rev Immunol 2014; 14(8):546–58. [PubMed: 25060580]
7. Alexopoulou L, Holt AC, Medzhitov R, Flavell RA. Recognition of double-stranded RNA and activation of NF-kappaB by Toll-like receptor 3. Nature 2001; 413(6857):732–38. [PubMed: 11607032]
8. Heil F, Hemmi H, Hochrein H, Ampenberger F, Kirschning C, Akira S, et al. Species-specific recognition of single-stranded RNA via toll-like receptor 7 and 8. Science 2004; 303(5663):1526–29. [PubMed: 14976262]
9. Kumagai Y, Takeuchi O, Akira S. TLR9 as a key receptor for the recognition of DNA. Adv Drug Deliv Rev 2008; 60(7):795–804. [PubMed: 18262306]
10. He WA, Berardi E, Cardillo VM, Acharyya S, Aulino P, Thomas-Ahner J, et al. NF-κB-mediated Pax7 dysregulation in the muscle microenvironment promotes cancer cachexia. J Clin Invest 2013; 123(11):4821–35. [PubMed: 24084740]
11. Talbert EE, Yang J, Mace TA, et al.: Dual Inhibition of MEK and PI3K/Akt Rescues Cancer Cachexia through both Tumor-Extrinsic and -Intrinsic Activities. Mol Cancer Ther 2017;16(2): 344–356. [PubMed: 27811010]

12. Casadei L, Calore F, Creighton CJ, et al.: Exosome-Derived miR-25-3p and miR-92a-3p Stimulate Liposarcoma Progression. Cancer Res. 2017;77(14):3846–3856. [PubMed: 28588009]
13. Tseng YC, Kulp SK, Lai IL, Hsu EC, He WA, Frankhouser DE, et al. Preclinical Investigation of the Novel Histone Deacetylase Inhibitor AR-42 in the Treatment of Cancer-Induced Cachexia. J Natl Cancer Inst 2015; 107(12): 1–14.
14. Paul KP, Gupta KS, Bhatnagar S, et al.: Targeted ablation of TRAF6 inhibits skeletal muscle wasting in mice. J Cell Biol 2010; 191(7): 1395–1411. [PubMed: 21187332]
15. Pyo JO, Yoo SM, Ahn HH, et al.: Overexpression of Atg5 in mice activates autophagy and extends lifespan. Nat Commun 2013;4:2300. [PubMed: 23939249]
16. Vande Velde C, Cizeau J, Dubik J et al.: BNIP3 and Genetic Control of Necrosis-Like Cell Death through the Mitochondrial Permeability Transition Pore. Mol Cell Biol 2000;20(15): 5454–5468. [PubMed: 10891486]
17. Talbert EE, Metzger GA, He WA, Guttridge DC. Modeling human cancer cachexia in colon 26 tumor-bearing adult mice. J. Cachexia Sarcopenia Muscle. 2014; 4:321–28.
18. Patel HJ, Patel BM. TNF-α and cancer cachexia: Molecular insights and clinical implications. Life Sci. 2017; 170:56–63. [PubMed: 27919820]
19. Fredrix EW, Soeters PB, Wouters EF, Deerenberg IM, von Meyenfeldt MF, Saris WH. Effect of different tumor types on resting energy expenditure. Cancer Res. 1991; 51:6138–41. [PubMed: 1657379]
20. Smith RC, Lin BK. Myostatin inhibitors as therapies for muscle wasting associated with cancer and other disorders. Curr Opin Support Palliat Care 2013; 7(4):352–60. [PubMed: 24157714]
21. Couch ME, Dittus K, Toth MJ, Willis MS, Guttridge DC, George JR, et al. Cancer cachexia update in head and neck cancer: Pathophysiology and treatment. Head Neck 2015; 37(7):1057–72. [PubMed: 24634283]
22. Martins T, Vitorino R, Moreira-Gonçalves D, Amado F, Duarte JA, Ferreira R. Recent insights on the molecular mechanisms and therapeutic approaches for cardiac cachexia. Clin Biochem 2014; 47(1-2):8–15. [PubMed: 24184665]
23. Kandimalla ER, Bhagat L, Wang D, Yu D, Sullivan T, La Monica N, et al. Design, synthesis and biological evaluation of novel antagonist compounds of Toll-like receptors 7, 8 and 9. Nucleic Acids Res 2013; 41(6):3947–61. [PubMed: 23396449]

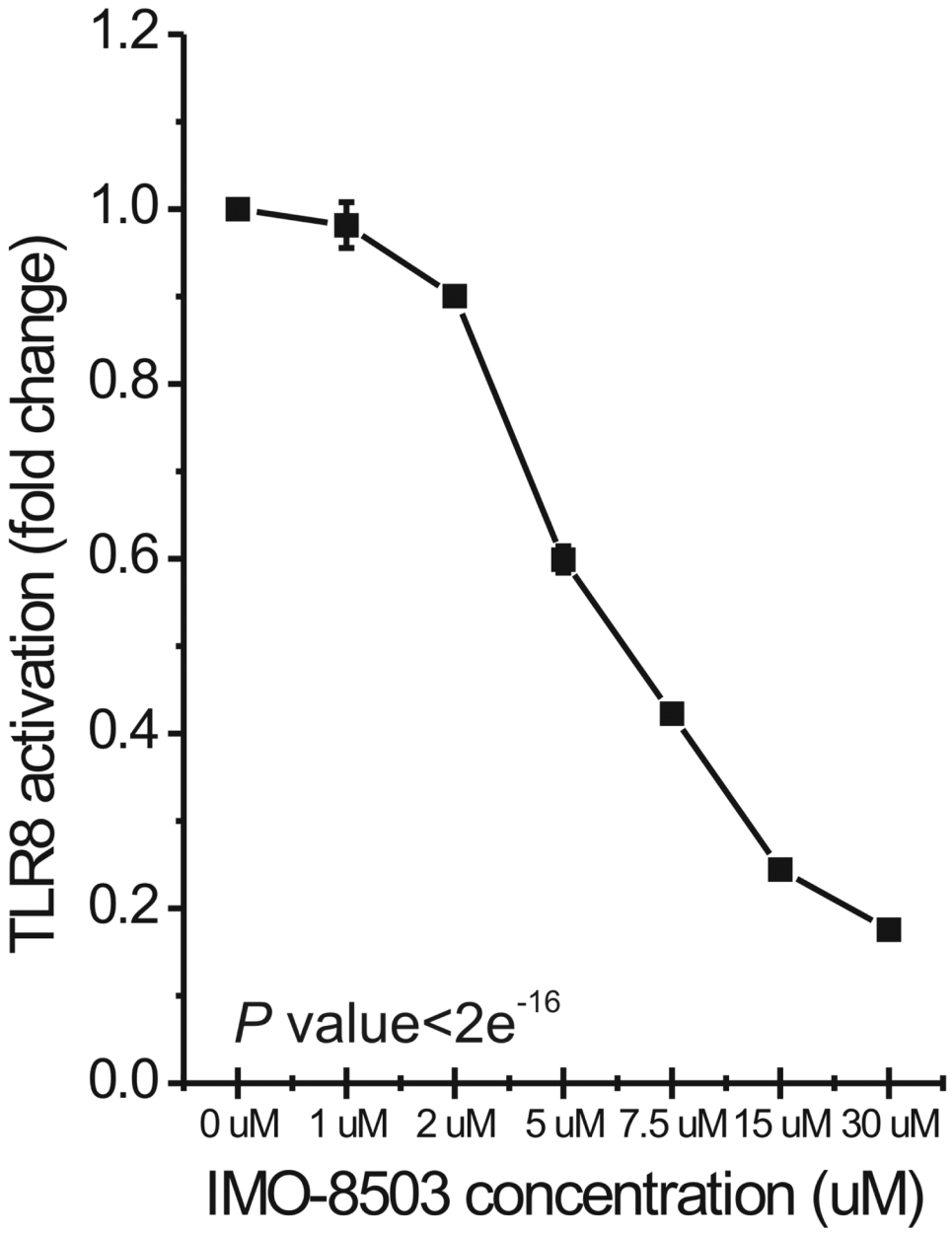

Figure 1. IMO-8503 impairs human TLR8 activation promoted by synthetic miR-21.

QUANTI-Blue assay performed on Human HEKBlue-TLR8 293 cells treated for 24h with Dotap formulation of miR-21 in the presence of the indicated concentrations of IMO-8503. Incubation with only miR-21 was used as positive control. Experiment was performed in triplicate. Results are presented as average ± S.D. Statistical analysis was performed by one-way ANOVA test.

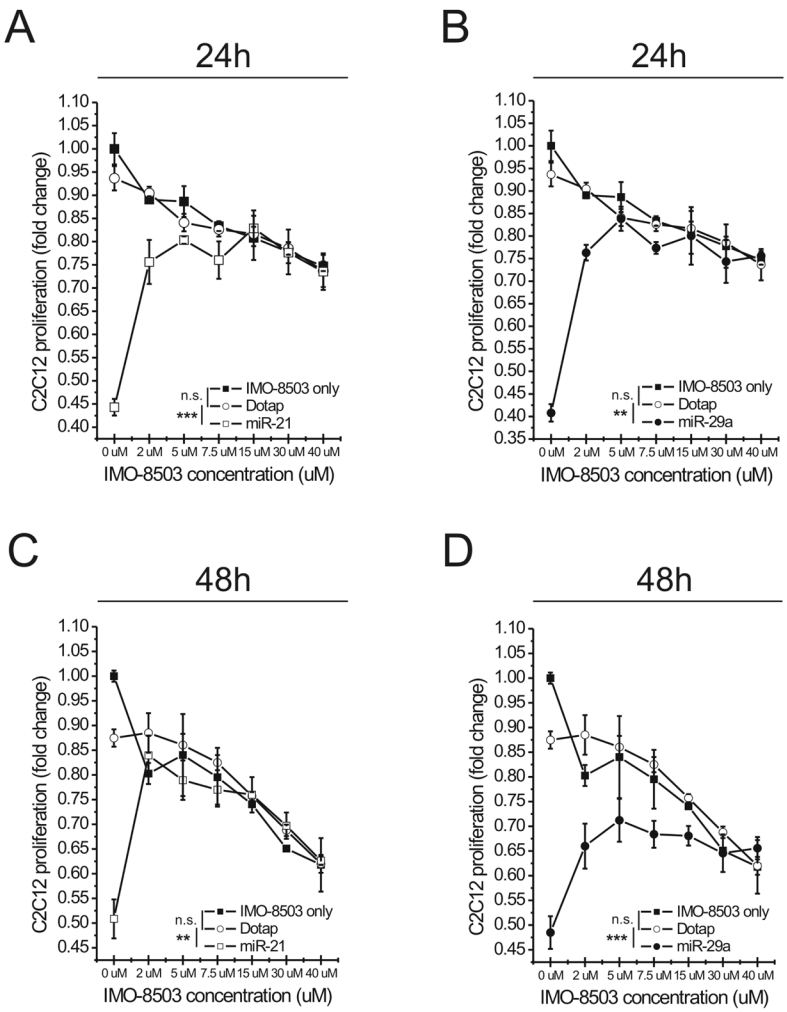

Figure 2. Pharmacological inhibition of *TLR7* with IMO-8503 protects C2C12 cells from cell death induced by synthetic miR-21 and miR-29a.

(A, B) C2C12 cells were treated with Dotap alone or Dotap formulations of miR-21 **(A)** and miR-29a **(B)** in the presence of increasing concentrations of IMO-8503. Cells were also treated with the indicated concentrations of antagonist only in order to assess the intrinsic toxicity of the molecule. After 24h cell proliferation was assessed through MTS assay. **(C, D)** The same assay was performed on C2C12 cells treated as described above for 48h. Results are presented as average ± S.D. Statistical analysis was performed by a two-way ANOVA test, in particular between the Dotap and IMO-8503 only conditions and between Dotap and miR-21/miR-29a conditions. n.s indicates “not significant”. **, $0.001 < P \leq 0.01$; ***, $P \leq 0.001$.

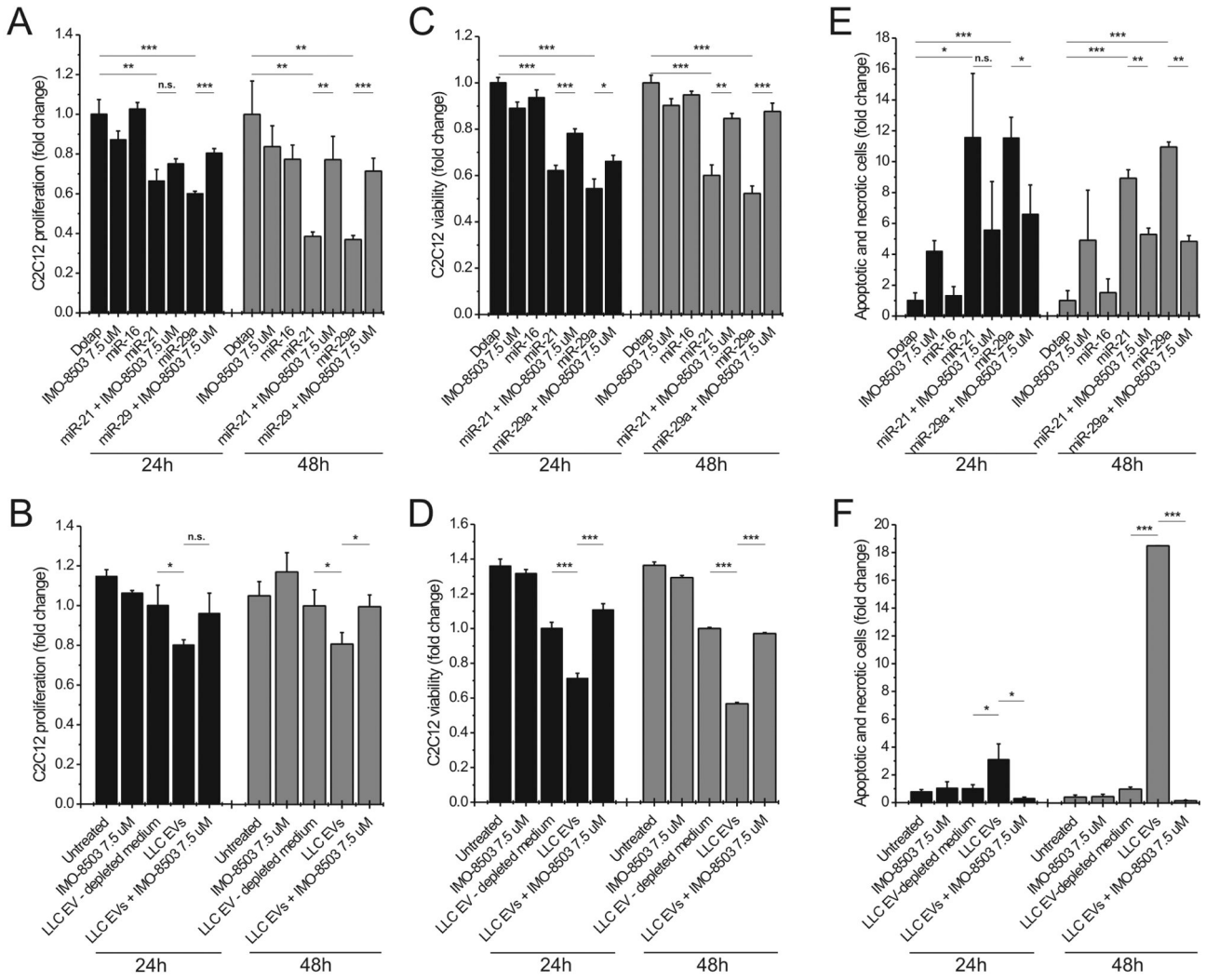

Figure 3. IMO-8503 protects C2C12 cells from apoptosis induced by exogenous miR-21/29a and by LLC-derived EVs.

(A) MTS assay performed on C2C12 cells treated for 24 (black) and 48h (grey) with Dotap alone or Dotap formulations of miR-16, miR-21 and miR-29a in the presence or absence of IMO-8503. Dotap alone and miR-16 were used as negative controls. **(B)** MTS assay performed on C2C12 cells incubated with LLC-derived EVs for 24 (black) and 48h (grey). EV-depleted medium (supernatant post-ultracentrifugation) was used as a negative control. **(C)** Trypan blue assay performed on C2C12 cells treated with Dotap formulations of miR-21 and miR-29a for 24 (black) and 48h (grey). Dotap alone and miR-16 were used as negative controls. **(D)** The same assay was performed on C2C12 cells incubated with LLC-derived EVs for the indicated time point. **(E, F)** Annexin-V and Propidium Iodide assay performed on C2C12 treated for 24h (black) and 48h (grey) with synthetic miRNAs **(E)** or LLC-derived EVs **(F)**. Results are presented as average ± S.D. T-test was used for statistical analysis. n.s indicates “not significant”. *, 0.01< $P \leq 0.05$; **, 0.001< $P \leq 0.01$; ***, $P \leq 0.001$.

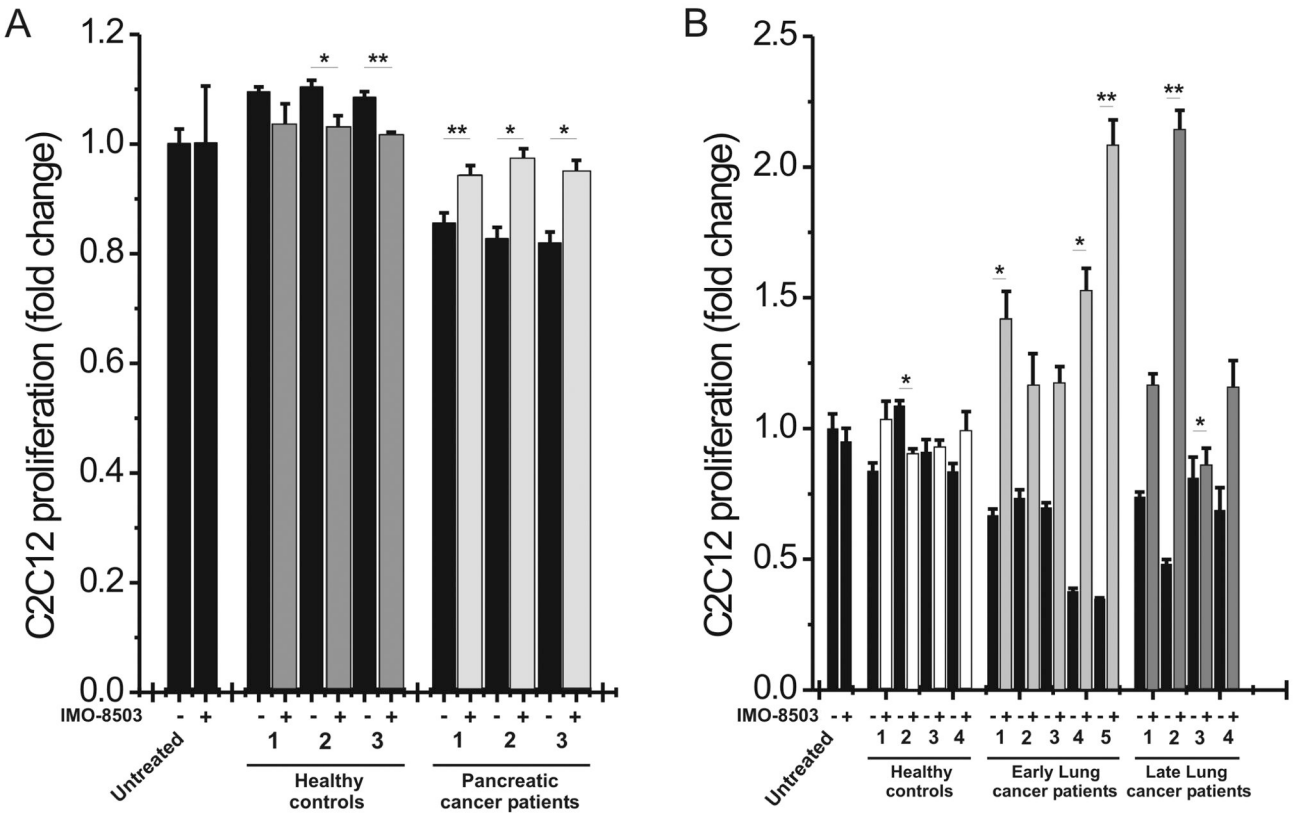

Figure 4. IMO-8503 impairs cell death induced by lung and pancreatic patient plasma-derived EVs.

(A) MTS assay performed on C2C12 cells treated for 24h with EVs isolated from the plasma of pancreatic cancer patients who suffered from cachexia. IMO-8503 was added where indicated at a concentration of 7.5 μM. As a control, C2C12 cells were treated in parallel with EVs isolated from the plasma of healthy donors. **(B)** Cell proliferation was assessed also for C2C12 cells treated with lung cancer plasma samples-derived EVs for 24h, in the presence or absence of IMO-8503. EVs were isolated either from the plasma of patients who suffered from lung cancer at an early stage, either from patients who were at a later stage. EVs derived from the plasma of healthy donors were used as negative control. Results are presented as average ± S.D. T-test was used for statistical analysis. *, $0.01 < P \leq 0.05$; **, $0.001 < P \leq 0.01$.

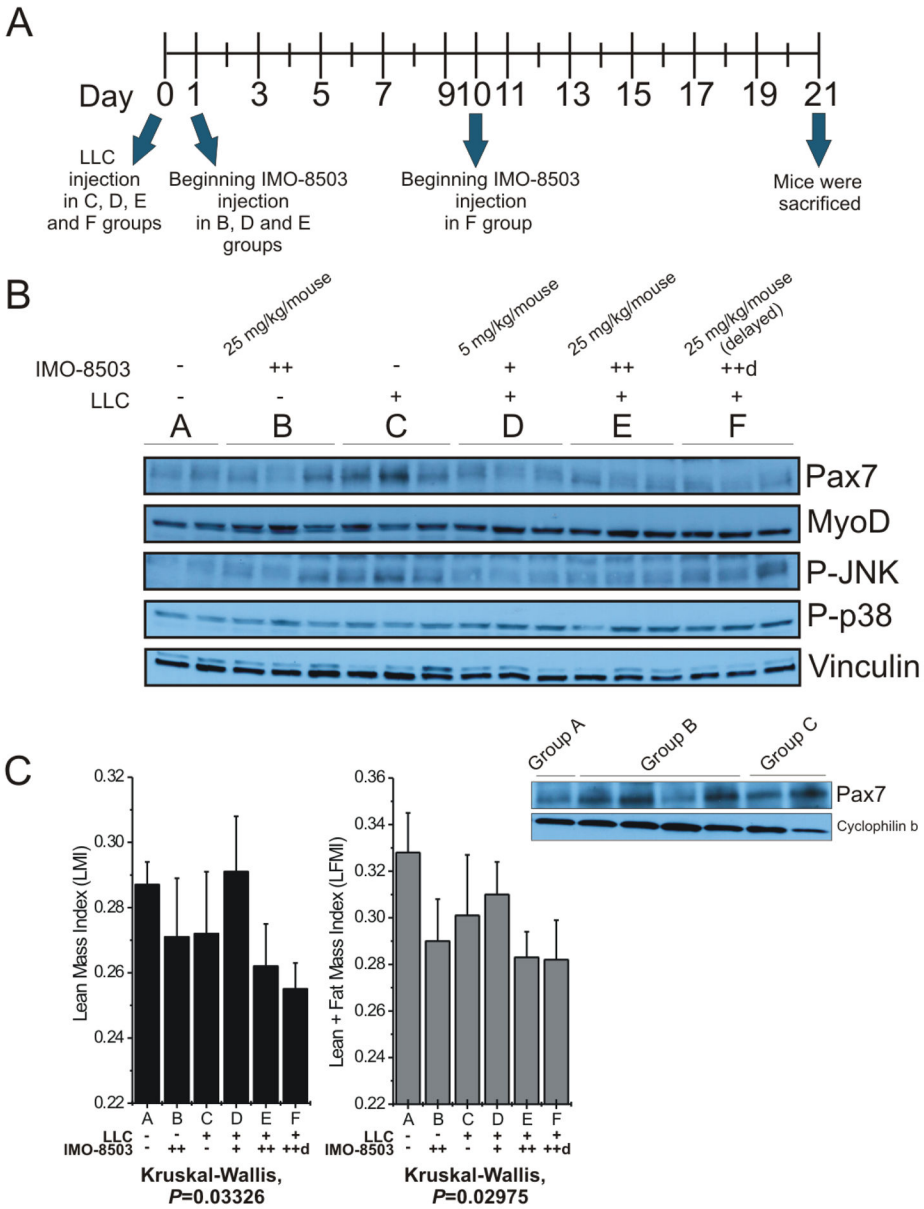

Figure 5. IMO-8503 treatment protects mice from LLC-induced cancer cachexia.

(A) Representative diagram of the *in vivo* experiment. **(B)** Immunoblotting for Pax7, MyoD, Phospho-JNK and Phospho-p38 performed on gastrocnemius lysates derived from C57/B6 mice injected with LLC cancer cells and treated with IMO-8503 as described in the Material and Methods section. Vinculin was used as a normalizer in order to show equal protein loading. All the gastrocnemius samples of the "B group" were separately analyzed for Pax7 expression in comparison to samples of Groups A and C (below). **(C)** Lean Mass Index (LMI, left panel) and (Lean + Fat) Mass Index (LFMI, right panel) were determined for mice whose body composition was analyzed through EchoMRI. +, 5 mg/kg/mouse; ++, 25 mg/kg/mouse; ++d, 25 mg/kg/mouse injected starting 10 days after LLC injection. Results are presented as average ± S.D.; Kruskal-Wallis rank sum test was performed for statistical analysis.

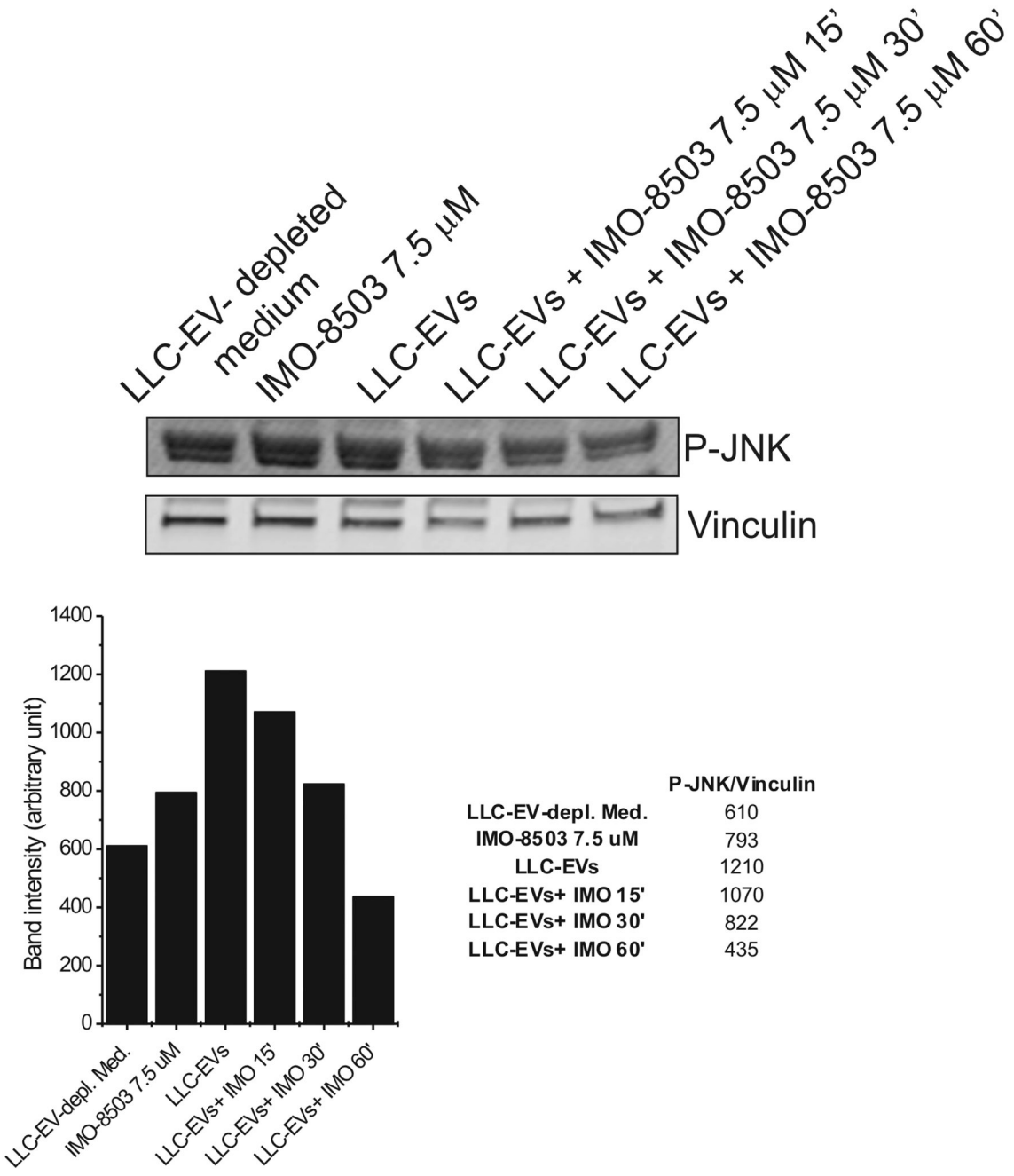

	P-JNK/Vinculin
LLC-EV-depl. Med.	610
IMO-8503 7.5 uM	793
LLC-EVs	1210
LLC-EVs+ IMO 15'	1070
LLC-EVs+ IMO 30'	822
LLC-EVs+ IMO 60'	435

Figure 6. Treatment with IMO-8503 impairs JNK phosporylation induced by LLC-derived EVs.

C2C12 cells were incubated for the indicated time points with LLC- derived EVs in the presence of IMO-8503 7.5 μM. Treatment with EVs only for 60' was used as positive control, while incubation for 60' with LLC-depleted medium represents our negative control.

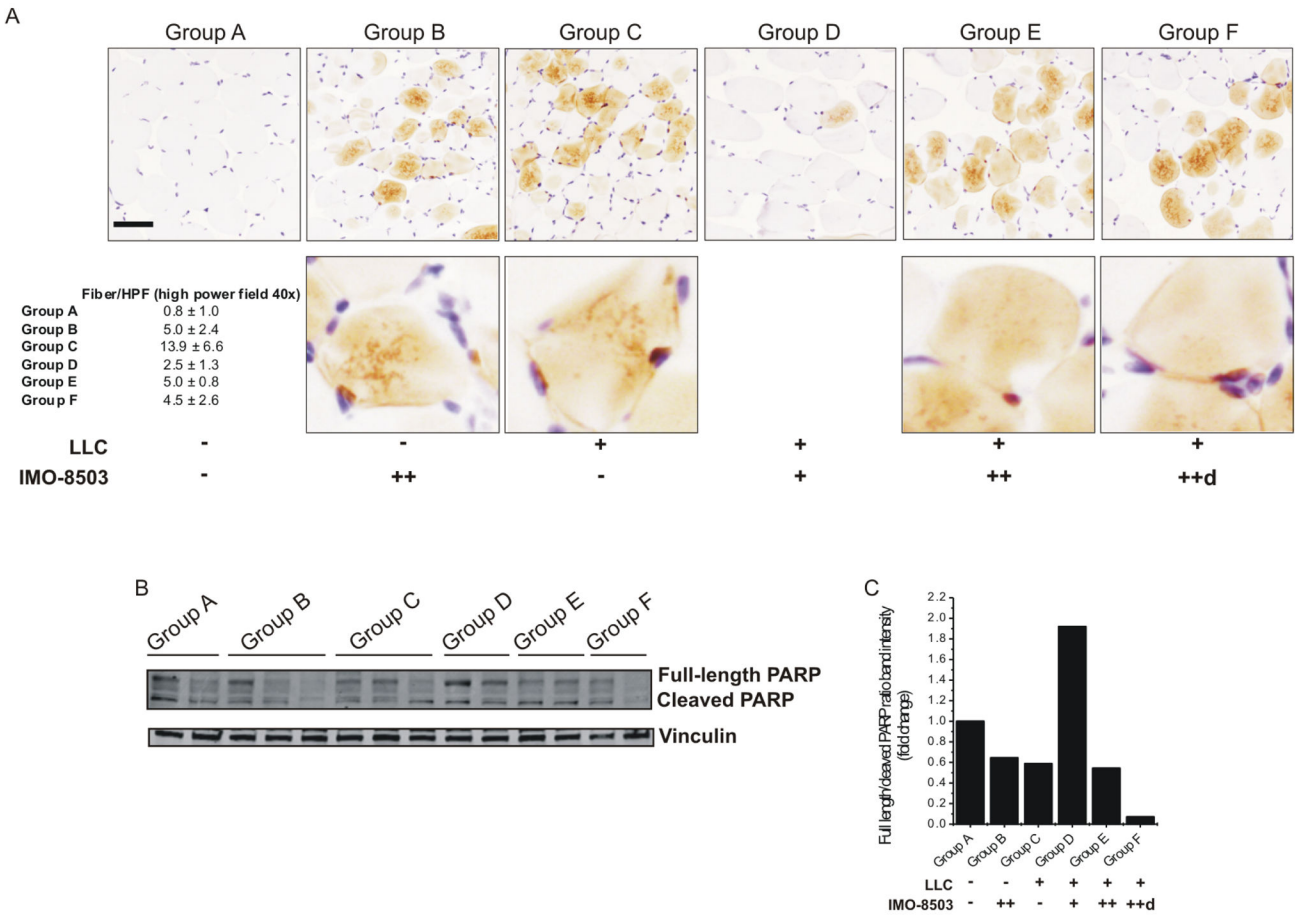

Figure 7. IMO-8503 impairs Caspase 3 and PARP cleavage in gastrocnemius when used at a dosage of 5 mg/kg/mouse.

(A) Isolated gastrocnemius muscles were processed for IHC in order to verify the cleaved Caspase 3 levels among all groups. Quantitation is shown as number of fibers per high power field (40X). Bar, 100 μm. The same samples were also processed for western blot analysis in order to assess the levels of PARP cleavage **(B)**. Ratio between full length and cleaved PARP bands for each group is shown in **(C)**.